

²⁵²Cf PLASMA DESORPTION MASS SPECTROMETRY. CONTRIBUTIONS FROM THE ROCKEFELLER UNIVERSITY *

BRIAN T. CHAIT

The Rockefeller University, 1230 York Avenue, New York, NY 10021 (U.S.A.)

(Received 31 August 1988)

ABSTRACT

The paper describes a selection of contributions made by members of Professor Frank H. Field's group in The Rockefeller University Mass Spectrometry Laboratory to both fundamental and applied aspects of ²⁵²Cf plasma desorption mass spectrometry.

INTRODUCTION

In 1974 Macfarlane and Torgerson [1,2] discovered a remarkable new method for the volatilization and ionization of involatile, thermally labile biomolecules. In their technique, molecular entities are desorbed and ionized directly from a solid surface by the passage of energetic ²⁵²Cf fission fragments through a surface coated with a compound of interest. The technique, which has come to be known as plasma desorption mass spectrometry (PDMS) or ²⁵²Cf fission fragment ionization mass spectrometry, has played a leading role in the emergence of mass spectrometry as an effective means for the characterization of underivatized biomolecules such as peptides, proteins, carbohydrates, and polynucleotides. Professor F.H. Field at The Rockefeller University was among the first members of the established mass spectrometric community to recognize the enormous potential value to biological research of the newly developed technique. He thus immediately initiated plans to construct a ²⁵²Cf fission fragment ionization mass spectrometer which was put into service in 1979 [3] and has been operating effectively and fruitfully up to the present time. This paper summarizes a selection of contributions made by the group at The Rockefeller University to both fundamental and applied aspects of the mass

* Dedicated to Professor Frank H. Field on the occasion of his retirement from Rockefeller University.

spectrometry of biomolecules using this ^{252}Cf fission fragment ionization mass spectrometer.

THE INSTRUMENT

The instrument which we constructed utilized a time-of-flight mass analyzer and was similar to that described by Macfarlane and Torgerson [4] but with some differences [5-8]. A schematic drawing of the apparatus is given in Fig. 1. The Rockefeller instrument has several noteworthy features, as follows.

The instrument incorporates a long (3 m) flight tube with an electrostatic particle guide [9] to enhance the transport efficiency of ions to the ion detector, as in the early Macfarlane and Torgerson design [4]. The long flight tube gives the mass analyzer an intrinsic resolution of ca. 2000 FWHM for ions with masses greater than 100 u, a mass determination accuracy of ca. 100 ppm, strong discrimination against energetic neutral fragments which are produced by metastable decomposition of ions during flight, and the opportunity to provide good immunity against noise from uncorrelated ions. These uncorrelated ions are generated by ^{252}Cf alpha particles, by the very high fields applied to the sample foil, and by fission fragments passing through the sample foil during a given timing cycle, subsequent to the fission fragment used to generate the time zero reference [10]. The elimination of these uncorrelated ions is achieved through the use of a set of pulsed deflection plates positioned just beyond the acceleration grids at the entrance to the flight tube (Fig. 1). A high voltage blocking potential is applied to these plates after the ions arising from a fission fragment of interest have been allowed to pass into the flight tube. Subsequently generated uncorrelated ions are then blocked for the remainder of the timing cycle.

The instrument incorporates a set of three accelerating grid electrodes positioned directly in front of the sample foil and three decelerating grid

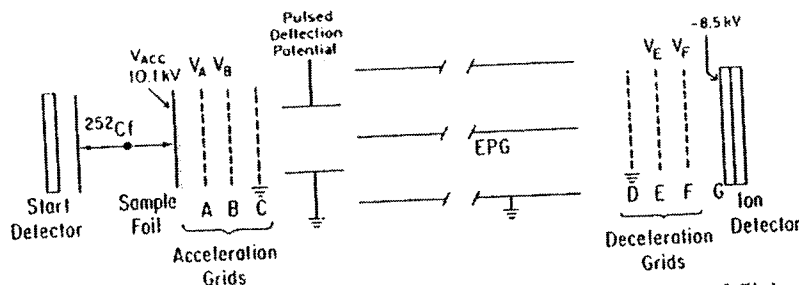


Fig. 1. Schematic representation of fission fragment ionization time-of-flight mass spectrometer. EPG is the electrostatic particle guide.

electrodes positioned just in front of the ion detector [11]. These grid electrodes allow us to study or to eliminate the ubiquitous metastable decomposition products which are an important feature of fission fragment mass spectra (see below).

Samples are inserted on a probe into the mass spectrometer through a vacuum lock with a insertion cycle time of ca. 1 min. This short cycle time is important, for example, when we wish to follow the progress of microchemical reactions taking place at the surface of solid samples (see below).

The ^{252}Cf source is purchased [12] as an electroplated layer (2 mm diameter) of californium oxide which is diffusion bonded to a 1 μm thick nickel foil and then sputter-coated with a thin layer of gold. During our initial handling of these ^{252}Cf sources, we found that it was desirable to sandwich the ^{252}Cf foil between additional 0.5 μm nickel foils to prevent self-sputtering escape of the californium [5]. Similar foil-sealed source assemblies can now be commercially acquired [12].

The time-of-flight measurements are made with a time-to-digital converter (TDC). No suitable commercially available TDC was available when we constructed our fission fragment instrument, making it necessary to design and construct a TDC in-house. The resulting device [8] has the following capabilities: time bin width, 5/8 ns; number of available time bins, $2^{21} = 2 \times 10^6$ (corresponds to a time span of up to 1.2 ms); multiple stop capability, 15 event times can be measured after a given start event; pulse pair resolution or deadtime, 7 ns; integral nonlinearity, less than seven parts in 10^7 . To make full use of these capabilities we have recently interfaced the TDC to a 32-bit MicroVax I computer [13], which can store a spectrum comprised of as many as 800 000 5/8-ns channels covering a time span of 500 μs , has a dynamic range of $0-2 \times 10^9$ events per time channel, and can read and store flight times in periods of the order of tens of microseconds [14].

FISSION FRAGMENT MASS SPECTRA—DECOMPOSITION MECHANISMS

When we put our fission fragment mass spectrometer into service, little was known about the excitation of the various species desorbed and ionized by the energetic ion bombardment, or the extent to which these desorbed species decomposed and the mechanisms by which this occurred. We thus undertook a detailed investigation of the complete positive and negative mass spectra and the decomposition mechanisms of ions produced from alanine, arginine, sucrose, guanosine, 5'-adenosine monophosphate, alanylalanine, and lysyltyrosylthreonine [5]. The spectra were obtained from samples introduced into the mass spectrometer in the form of thin solid films produced by electrospray deposition [15]. The mass-to-charge ratios

were measured with sufficient precision to permit deduction of atomic compositions for many of the observed fragment ions. The significant findings of the study were as follows.

(1) The amount of fragmentation occurring in fission fragment ionization even for the relatively simple molecules included in the study was large. Thus relatively low intensities of quasi-molecular ions were observed and many small fragment ions were produced with large intensities. For example, only for alanine was the intensity of the quasi-molecular ion greater than 10% of the total ionization, and for arginine the CN^- ion comprised 56% of the total negative ionization. Thus the amount of energy transferred to a large proportion of the molecules undergoing ionization must have been relatively large, and we concluded that the technique should not be looked upon only as a soft ionization method. Rather, the method appears to have a dual character with desorption and ionization involving two modes: a gentle one which produces intact quasi-molecular ions and a violent one which produces, for example, the kind of fragmentation that in the case of negative ions reduces guanosine extensively to CN^- ions.

(2) Much of the fragmentation that occurs could be rationalized in terms of established concepts of gaseous-ion chemistry. Both the positive and negative ion spectra contained mostly even-electron ions which appeared to be produced by chemical ionization-like processes and gave rise to many structurally significant fragment ion species. Thus, for example, the positive-ion spectrum of the tripeptides gave rise to the structurally informative types of ions observed earlier by Field and co-workers [16] in their study of peptide sequencing by isobutane chemical ionization.

Our first application of ^{252}Cf PDMS which used the findings outlined above involved a study of the 20-residue pore-forming peptide antibiotic alamethicin [6]. Some controversy had surrounded the elucidation of the structure of natural alamethicin, which is a mixture of closely related compounds. The study was undertaken in collaboration with Professor B.F. Gisin, who synthesized several candidate structures for the major component of alamethicin, alamethicin I. He found that one of these synthetic peptides (Fig. 2) was identical to the natural alamethicin I by a series of different criteria which included amino acid analysis, high-performance liquid chromatography, nuclear magnetic resonance spectroscopy, and biological activity. It was, however, not possible to compare the sequences directly using Edman sequence analysis because of the blocked amino-termini. We thus compared, in detail, the positive and negative ^{252}Cf fission fragment ionization mass spectra of natural and synthetic samples of alamethicin I (Fig. 3). In addition to providing molecular weight information, the positive ion spectra were found to provide detailed information on the amino acid sequences of the peptides. The close identity of these positive

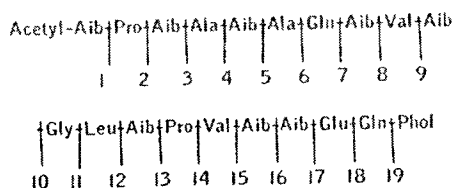


Fig. 2. Amino acid sequence of synthetic alamethicin I. Monoisotopic molecular weight = 1963.1. Aib; aminoisobutyric acid; Phol, phenylalaninol.

ion spectra from the natural and synthetic peptides then provided strong evidence that the natural and synthetic samples were indeed identical and that natural alamethicin I has the same structure as the known structure of the synthetic sample. Reaction mechanisms leading to the production of the several series of sequence ions were suggested. The chemical identities of the ions which comprise the series were again the same as or analogous to the amino terminal ions observed previously in the isobutane chemical ionization mass spectra of peptides [16] and which have come to be known as the A, B and C series in the most recent nomenclature [17]. Two of the sequence

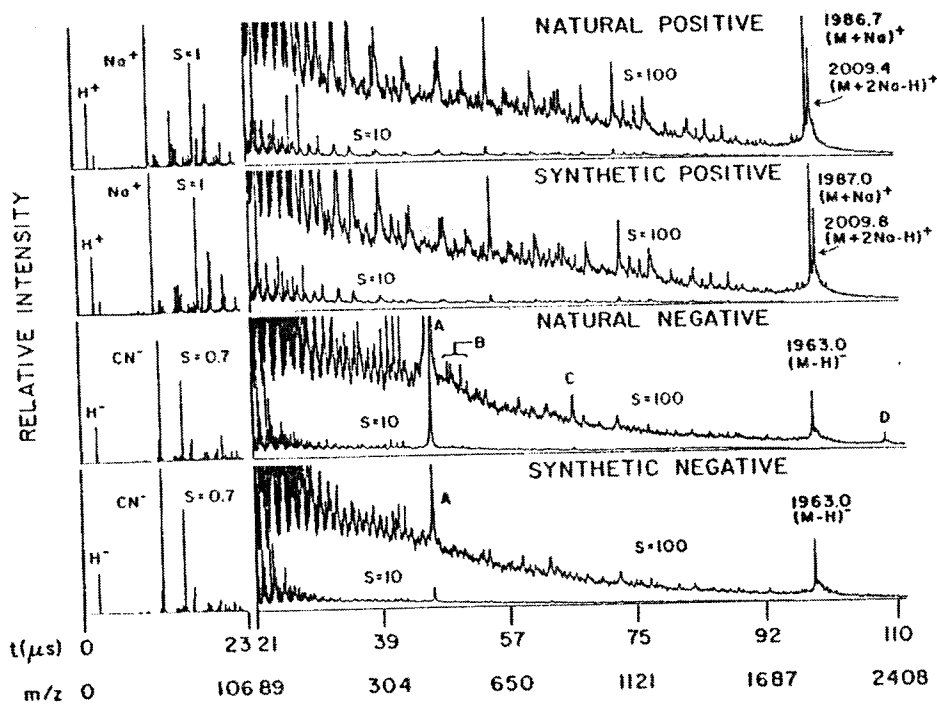
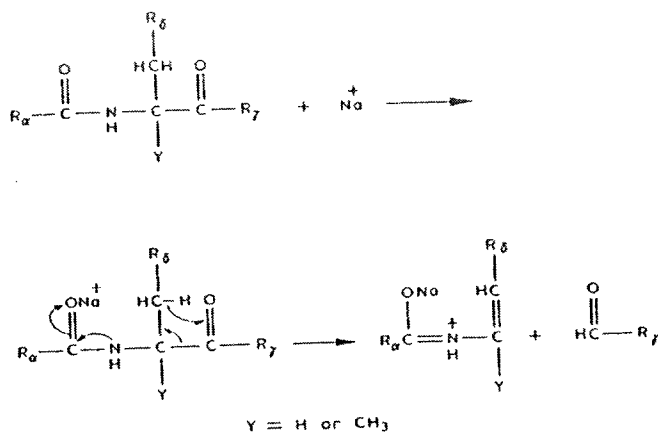


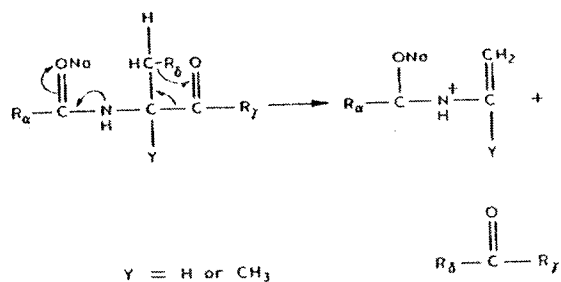
Fig. 3. Spectra of alamethicin I. S = sensitivity of intensity display. Peaks A, B and C in negative ion spectra arise from an anionic detergent impurity.



Scheme 1.

ion series (which had not previously been described) involved the addition of a sodium ion to the alamethicin I molecule followed by fragmentation with retention of the sodium in the charged fragment. The suggested reaction mechanism which leads to the most extensive series of sequence ions is given in Scheme 1. This imine fragment ion series included ions formed by breaking each of bonds 1-17 with only one exception. The ion formed by breaking bond 11 was absent from the sequence. The residue to the left of this bond is glycine, and we ascribed the absence of the ion to the fact that glycine has no hydrogen that can take part in the four-center decomposition depicted in Scheme 1.

We also observed five imine series ions produced by a variant of this reaction, as shown in Scheme 2. These variant imine fragmentations were found to occur at each residue where the component of the amino acid sidegroup R (Scheme 2) is an entity larger than H. The upper limit with this fragmentation was at bond 18.



Scheme 2.

In summary, the reactions shown in Schemes 1 and 2 gave rise to sequence information complete except for ions formed by breaking bonds 11 and 19. The identity of the fragmentation spectra from natural and synthetic alamethicin I then provided strong evidence for the detailed sequence identity of the two compounds.

METASTABLE DECOMPOSITIONS

^{252}Cf mass spectra have a distinct and unusual appearance; the spectral peaks are frequently exceedingly broad and often have complex shapes. The unusual appearance of the spectra undoubtedly contributed to the slow acceptance of PDMS as a useful analytical tool. When we put our instrument into service these dominating spectral features were unexplained. We thus initiated a study of the factors affecting the peak shapes observed in our time-of-flight instrument for a series of compounds including alanylalanylalanine, guanosine, 5'-adenosine monophosphate, erythromycin, and chlorophyll *a* [7]. We hypothesized and subsequently confirmed that a major cause of the broadening is the metastable decomposition of ions in flight, with the release of internal energy as kinetic energy. Two lines of investigation were pursued to test this hypothesis. In one, the residence time of ions in the acceleration zone between the sample foil and the first acceleration grid (Fig. 1) was varied by applying appropriate potentials to the first acceleration grid. By studying the high-time tails and the peak intensities as a function of residence time we were able to detect and measure abundant unimolecular fragmentation reactions occurring within a period 5–100 ns after ion formation. In the other line of investigation, metastable fragments were separated from their parent ions on the basis of their different kinetic energies. This was accomplished by using a set of deceleration grid electrodes placed directly in front of the ion detector at the end of the flight-tube (Fig. 1). Figure 4 shows the results of this latter type of investigation obtained on the $(\text{M} + \text{H})^+$ and $(\text{M} + \text{Na})^+$ ions from the tripeptide AlaAlaAla (MW = 231). The spectrum shown in Fig. 4A was obtained with no potential applied to the deceleration grids and gives the normal time-of-flight spectrum of the compound. Under these experimental conditions, fragment ions and neutral species arising by metastable decomposition in the field-free flight tube have the same mean velocities as the precursor ions from which they arise. Thus the neutral and charged fragments contribute to the same peak in the velocity measuring time-of-flight instrument as do their unfragmented precursor ion species.

It is seen from Fig. 4A that the peak corresponding to the protonated molecule is substantially broader than that of the sodium-cationized species, which has a width consistent with the limiting instrumental resolution of ca.

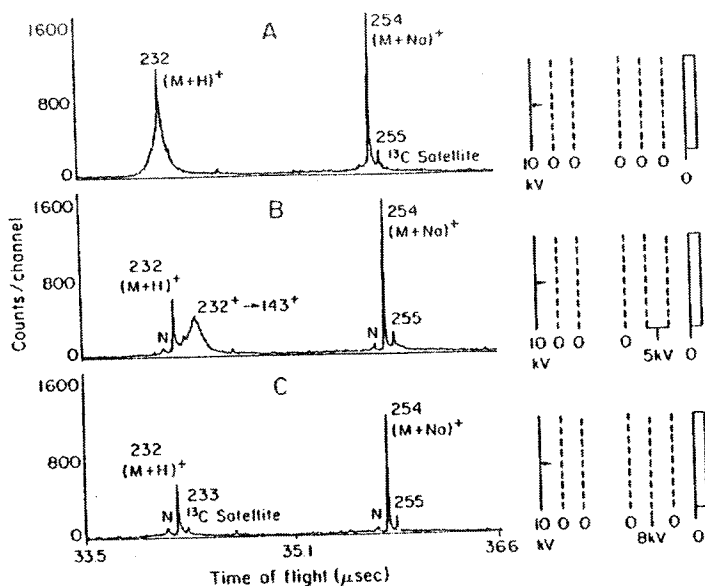


Fig. 4. Quasi-molecular ion peaks in alanylalanylalanine; $(M+H)^+$ and $(M+Na)^+$ peaks at three decelerating potentials: A, 0 V; B, 5 kV; and C, 8 kV.

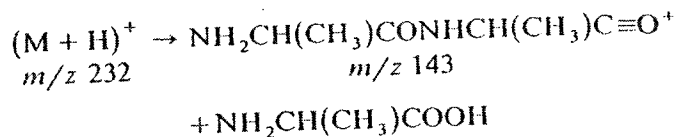
2000 FWHM. The reason for the large width of the $(M+H)^+$ peak is apparent from Fig. 4B, where the applied deceleration potential has caused the original broad peak to split into three components. The small peak, labeled N, corresponds to the unretarded neutral entities. The large sharp peak corresponds primarily to unfragmented $(M+H)^+$ ions, and the broad peak corresponds to $(M+H)^+$ ions which have undergone metastable fragmentation in the field-free flight tube. As the deceleration potential is further increased, the metastable decay product ions have increasingly longer flight times with respect to the unfragmented parent ions, and they are finally suppressed altogether as shown in Fig. 4C.

In addition to providing an explanation for the origin of the broad and complex peaks observed in PDMS, several useful pieces of information on the excitation and fragmentation of ion species desorbed by fission fragments could be deduced from these and similar retardation experiments:

(1) Sodium cationization was in general shown to inject less energy into the desorbed molecule than protonation, or at least produced ions which underwent less metastable fragmentation. Thus, 82% of the $(M+H)^+$ ions of AlaAlaAla were observed to undergo flight-tube fragmentation reactions versus only 46% for the $(M+Na)^+$ species.

(2) The retardation behavior of the metastable components with respect to the precursor ion was used to deduce information on the identities of the

fragmentation pathways. Thus, for example, protonated AlaAlaAla could be shown to decay in the flight tube primarily through the single transition



(3) The time spreads of the separated metastable components were used to deduce lower limits for the average amount of internal energy that was converted into translational energy for given metastable transitions. Thus, for example, a lower limit of 32 ± 9 meV was measured for the energy release which occurred during the metastable transition $232^+ \rightarrow 143^+$ shown above.

(4) From a practical point of view we demonstrated (see, e.g. Fig. 6) that the suppression of decomposition products can be used to enhance the resolution by eliminating the broad components of the peaks or separating them from the sharp components.

In an effort to widen our understanding of the behaviour of large ionized molecules produced by fission fragment bombardment, we undertook a detailed investigation of the fragmentation of chlorophyll *a* (Chl *a*), MW = 892 [11,18,19]. The normal fission fragment time-of-flight mass spectrum of Chl *a* (Fig. 5A) showed that a very high proportion of the ionized molecules undergo prompt fragmentation reactions (reactions occurring in times $< 10^{-8}$ s after the ionizing events that give rise to the sharp fragment ion peaks). The normal mass spectrum shown in Fig. 5A gives a "snapshot" of the distribution of ions formed from Chl *a* ca. 100 ns after the ion-forming event (the time required to accelerate the ions into the field-free flight tube). This "snapshot" is somewhat blurred by the subsequent metastable decomposition of many of these ions. Figure 5B shows the equivalent spectrum after all metastable fragmentation products (those fragments produced in times between 10^{-7} and 10^{-4} s after the ionizing event) have been removed. Only 22% of all ions in the mass range 400-1000 and only 1.1% of the M^{++} and $(M + H)^+$ species survive the flight to the detector. The low survival rate can be seen in Fig. 6, which shows the molecule ion region of a chlorophyll *a* sample containing a small amount of pheophytin *a* (Pheo *a* = Chl *a* - Mg + 2H). In this measurement the broad metastable peaks (shown cross-hatched) have been separated from the sharp peaks which arise from ions not fragmenting in the flight tube. By measuring the time separation t between the broad metastable peak and its sharp precursor peak we could determine the mass of the metastable daughter ion [11,18]. In the case shown, the neutral loss from both Chl *a* and Pheo *a* was determined to be 279 ± 2 u, corresponding to the elimination of the phytol hydrocarbon tail.

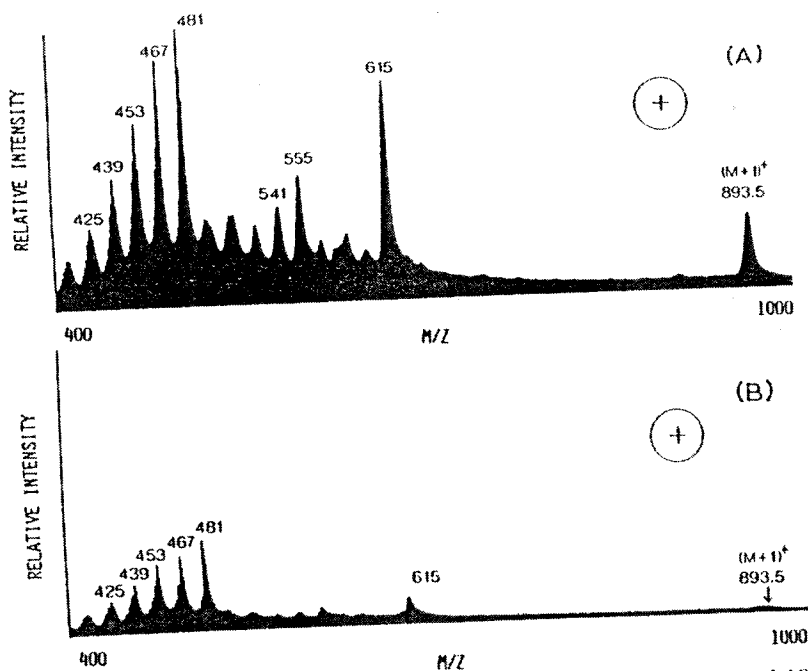


Fig. 5. Positive ion mass spectra of chlorophyll *a* between m/z 400 and 1000. A, spectrum taken with deceleration potential = 0. B, Spectrum taken with deceleration potential = 99% of acceleration potential.

In this way we obtained maps of most of the intense metastable fragmentation in Chl *a* for both positive (Fig. 7) and negative ions, and were able to show that much of the fragmentation could be readily rationalized by using well-known concepts of gaseous ion chemistry. Rate constants for certain

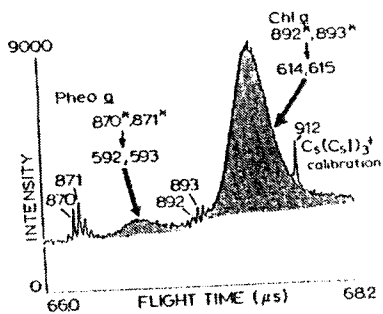


Fig. 6. Quasi-molecular ion peaks from chlorophyll *a* sample containing a small admixture of pheophytin *a*. Separation of broad peaks arising from flight-tube fragmentation products (cross-hatched) and sharp peaks arising from ions not undergoing fragmentation. The metastable transitions are indicated.

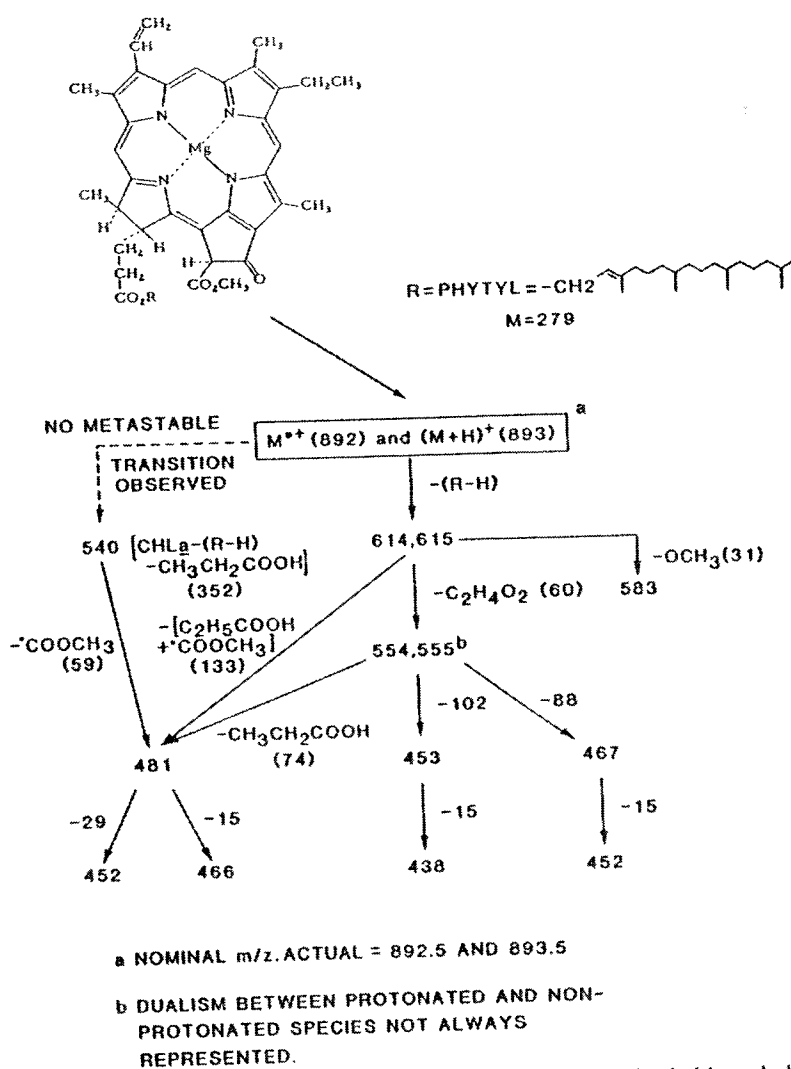


Fig. 7. Map of positive ion flight-tube fragmentation of ionized chlorophyll *a*.

fragmentation reactions were deduced from tails of peaks and from measurements which used segmented fields in the ion acceleration region. We found that fragmentation occurs with rate constants ranging from $> 10^9 \text{ s}^{-1}$ to 10^4 s^{-1} , and we suggested that the fission fragment induced fragmentation processes observed in Chl *a* involved many of the concepts embodied in the quasi-equilibrium theory of mass spectra, e.g. formation of reactant ions with a wide range of energies, which results in a network of sequential

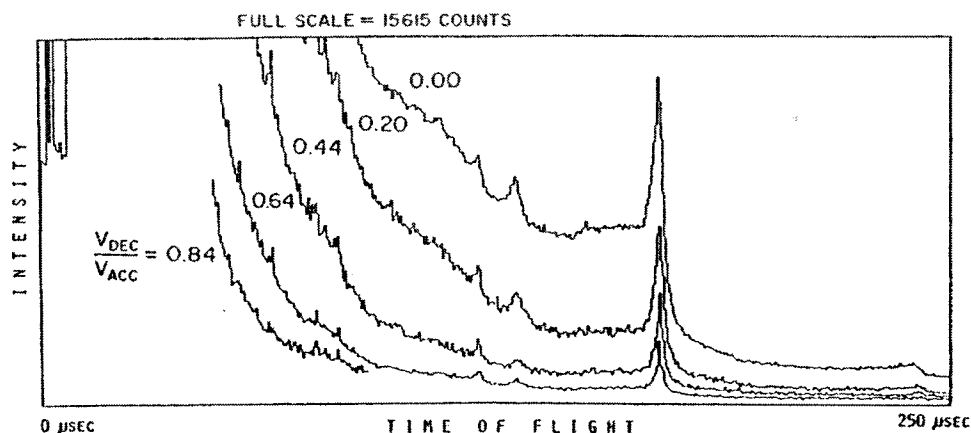


Fig. 8. Time-of-flight spectra of bovine insulin with five different magnitudes of the ratio of the deceleration potential to the acceleration potential, V_{dec}/V_{acc} . The run at 0.84 is only represented up to 90 μ s for the sake of clarity.

and competing unimolecular reactions with variable and wide-ranging rate constants.

The studies described above were made on compounds with molecular weights less than 1000 u. Larger molecules are, in general, more difficult to volatilize than are smaller molecules and may therefore be expected to absorb more energy during desorption. On the other hand, larger molecules contain many more degrees of freedom and can therefore absorb more energy without undergoing fragmentation than can smaller species. To investigate the competition between these opposing effects, we extended the investigation of the metastable decomposition of fission fragment bombardment produced ions to a considerably higher molecular weight compound, i.e. the polypeptide hormone bovine insulin, which has a monoisotopic molecular weight of 5729.6 [20]. Metastable fragmentation measurements were made of the decay of the $(M + H)^+$ ion, the $(M + 2H)^{2+}$ ion, the $(2M + H)^+$ ion, intact A- and B-chain fragment ions, and ions constituting the intense continuum observed in the positive fission fragment induced mass spectrum. Figure 8 shows the effect on the time-of-flight mass spectrum of applying a series of potentials to the metastable rejection grids at the end of the flight tube (Fig. 1). Ion fragments with

$$M(\text{fragment}) < (q_D V_{dec} / q_A V_{acc}) \times M(\text{precursor}) \quad (1)$$

where q_A is the charge on the accelerated ion, q_D is the charge on the decelerated ion, V_{dec} is the deceleration potential, and V_{acc} is the acceleration potential, are reflected and are thus not detected. Clearly, both the peaks and the continuum become smaller as larger deceleration potentials are

applied, corresponding to the rejection of increasing amounts of flight-tube fragmentation products. The data indicated that only a very small percentage ($< 4\%$), of the insulin dimer ions which survive acceleration ($t_{acc} = 539$ ns) subsequently survive the $240 \mu\text{s}$ flight to the detector. Similarly, $< 10\%$ of the protonated molecule ions which are still intact after 381 ns survive the remaining $170 \mu\text{s}$ flight to the detector. Almost half of the $(M + H)^+$ ions decay in flight to fragment ions with $m/z < 1200$. We hypothesized that many of these low-mass fragment ions are formed by sequential decay processes, as a single decay is not likely to reduce significantly the energy content per degree of freedom of a heavy fragment compared with its high-mass precursor [19]. Indeed, the A- and B-chain prompt fragment ions were found to have a similar propensity to undergo metastable decompositions as do the $(M + H)^+$ ions.

An investigation of the temporal distribution of the flight-tube fragmentations also indicated that the decays are heavily weighted to favor early times, i.e. high rate constants.

In 1985 Sundqvist, Roepstorff and co-workers [21] devised a new method for polypeptide sample preparation which yielded fission fragment mass spectra of much higher quality than that previously obtained with samples produced by electrospray deposition. The method involves the non-covalent attachment of monolayer amounts of polypeptide to a supporting matrix of nitrocellulose (NC) which has an affinity for the polypeptide. The results of these workers indicated that protonated polypeptides desorbed from NC undergo substantially less fragmentation than do polypeptides desorbed from bulk material. A strong enhancement of multiply charged (protonated) intact molecule species was also observed from NC. Two further practical benefits resulted from the use of NC. First, the sensitivity for detecting polypeptides was increased by several orders of magnitude. Second, the sensitivity of the spectral response to impurities (e.g. salts) was markedly reduced because the impurities could frequently be removed from the surface-sorbed polypeptide layer by simply rinsing the surface with clean solvent. In the hope of casting some light on the physico-chemical reasons for the improvements observed with NC, we undertook a series of comparisons between the amount of fragmentation in ions desorbed from bulk (electrosprayed) polypeptide samples and the amount of fragmentation observed in the corresponding ions desorbed from polypeptides bound to NC [22]. Figure 9 gives a comparison between the mass spectra obtained from an electrosprayed sample of porcine insulin (MW = 5777.7 u) (Fig. 9A) and NC-bound sample (Fig. 9C). Both these spectra were obtained with the deceleration grids (V_d in Fig. 1) set to the flight-tube potential (0 V). Under these conditions no ions which undergo metastable decomposition in the flight tube are rejected [19] so that these spectra give "snapshots" of the ion

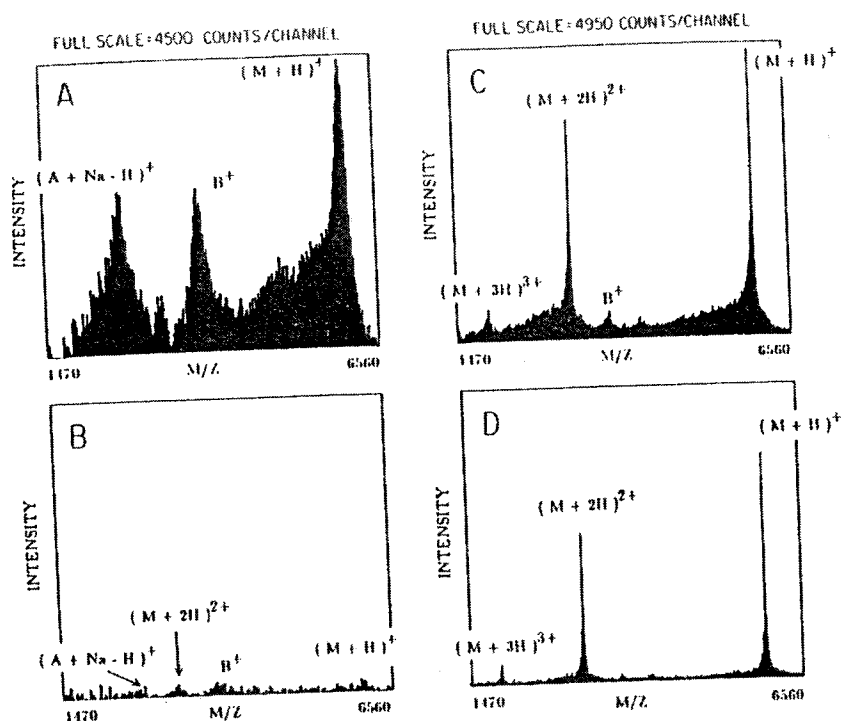


Fig. 9. Partial time-of-flight mass spectra of porcine insulin. A, Electro sprayed sample. No metastable suppression applied, $V_{\text{dec}}/V_{\text{acc}} = 0.0$ kV/10.0 kV. Run time = 287 min. B, Electro sprayed sample. Metastable suppression applied, $V_{\text{dec}}/V_{\text{acc}} = 8.4$ kV/10.0 kV. C, Nitrocellulose-bound sample. No metastable suppression applied, $V_{\text{dec}}/V_{\text{acc}} = 0.0$ kV/10.0 kV. Run time = 61 min. D, Nitrocellulose-bound sample. Metastable suppression applied, $V_{\text{dec}}/V_{\text{acc}} = 9.0$ kV/10.0 kV.

populations in the time range between 2×10^{-7} s and 4×10^{-7} s after the ion-forming event. To accentuate the ion peaks, the smooth, featureless continua were subtracted from these spectra. Comparison of Fig. 9A and 9C revealed several striking differences between the spectra obtained using the two different sample preparation techniques. The spectrum obtained with the NC-bound sample exhibits much sharper peaks, a much smaller intensity of fragment ion species, a lower intensity of ions comprising the broad features between the various peaks, and a considerably higher intensity of doubly and triply charged (protonated) intact peptide ions. The data shown in Fig. 9A and 9C are consistent with a considerably lower-energy injection into the protonated porcine insulin ions desorbed from NC compared with the corresponding ions desorbed from bulk electro sprayed layers. Further information on the relative degree of excitation of insulin ions desorbed from the two different sample preparations was obtained by a study of the

metastable fragmentation of the ions during transit through the 3-m flight tube. Such flight tube fragmentation reactions occur for the $(M + H)^+$ ion at times greater than 3.8×10^{-7} s but less than 1.7×10^{-4} s after the ion-forming event. The spectrum shown in Fig. 9B was obtained from the same electrosprayed sample as that shown in Fig. 9A except that a potential was applied to the deceleration grid E (Fig. 1) sufficient to reject the majority of ions which undergo fragmentation in the flight tube. Clearly, very few ions which survive acceleration survive their subsequent transit of the flight tube, e.g. only 2.6% of $(M + H)^+$ ions. This finding is in sharp contrast to the observed survival rate of porcine insulin ions desorbed from NC. Figure 9C shows the partial spectrum from NC-bound insulin with no metastable suppression, and Fig. 9D shows the corresponding spectrum from the same sample with metastable suppression. Again, the ions constituting the broad features between the discrete peaks largely disappear. The $(M + H)^+$ ions, however, have in this case a measured survival rate of fully 78%. These data provided striking evidence that protonated insulin molecules desorbed from NC contain considerably less internal energy than do the corresponding species desorbed from bulk insulin. The detailed reasons for the reduced excitation from NC remain to be elucidated. However, as previously suggested [21,23,24], reduction of the binding energy of the molecules of interest to other molecules and to the surface is probably the dominant factor. Improvements in our undertaking and control of the binding of biomolecules to surfaces holds the prospect of increasing our control over the amount and type of fragmentation incurred during desorption.

We also found that the relative survival probability of polypeptide ions desorbed from NC by fission fragments decreases as a function of increased polypeptide molecular weight. Thus, the injection of an excessive amount of energy during the ion-induced desorption and ionization processes still severely limits the quality of mass spectra obtained from polypeptides with molecular weights > 10000 u, as can be seen, for example, from the partial mass spectrum of horse heart cytochrome C (MW = 12361 u) shown in Fig. 10A.

In addition, we were able to demonstrate, for the first time, that a substantial fraction of the slow unimolecular fragmentation reactions of multiply protonated polypeptides gives rise to two charged fragmentation products rather than a multiply charged fragment and a neutral fragment. This finding confirmed our expectation, based on general energetic and statistical considerations, that the multiple charges would frequently be shared between the fragmentation products. Figure 10B shows the spectrum of fragmentation products which arise exclusively from dissociation of multiply protonated parent molecule ions into two charged fragments. All other ions have been excluded from this mass spectrum by the application of

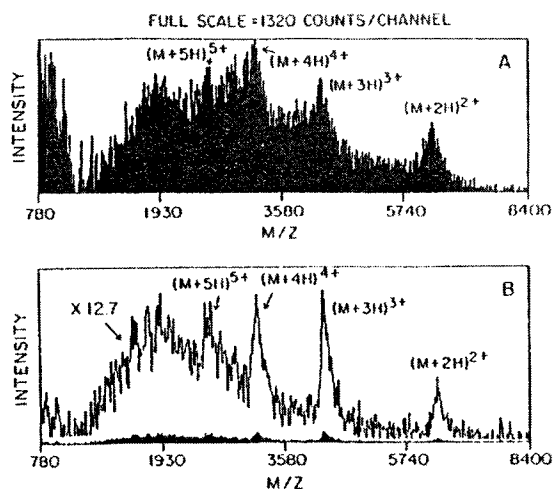


Fig. 10. Time-of-flight mass spectra of horse heart cytochrome C deposited on nitrocellulose showing the region containing the multiply protonated ion peaks. A, No metastable suppression applied, $V_{\text{dec}}/V_{\text{acc}} = 0.0$ kV/5.0 kV. B, Metastable suppression applied, $V_{\text{dec}}/V_{\text{acc}} = 5.3$ kV/5.0 kV. Filled-in spectrum has been normalized in time with respect to the spectrum shown in A. Unfilled-in spectrum is magnified in intensity by a factor of 12.7 compared with the filled-in spectrum.

a potential (V_{dec}) to the deceleration grid with a magnitude greater than that of the acceleration potential (V_{acc}) (see Eq. 1).

COMPARISON OF MASS SPECTRA OBTAINED WITH MeV AND keV ION BOMBARDMENT

Shortly after ²⁵²Cf fission fragments with energies of ca. 100 MeV were shown to be highly effective for desorption and ionization of involatile molecules [1,2], Benninghoven and co-workers [25–27], using a magnetic deflection instrument, demonstrated that ions with energies four orders of magnitude lower than fission fragments (i.e. a few keV) were also effective for production of ionized gas-phase molecules from organic solids, at least for compounds with molecular weights < 300 u.

In 1980, together with Standing and Ens at the University of Manitoba, we undertook to compare closely the relative properties and merits of these two techniques [28] by obtaining mass spectra of a series of compounds using the same samples mounted on the same sample foils in two similar time-of-flight mass spectrometers, the Rockefeller University fission fragment instrument (described earlier in this paper) and the pulsed keV ion bombardment mass spectrometer constructed by Chait and Standing at the University of Manitoba [29]. No direct comparison of this type had previ-

